ELSEVIER

Chemical Engineering Journal 84 (2001) 343–354

Chemical Engineering Journal

www.elsevier.com/locate/cej

Comparison of aerodynamics and mixing mechanisms of three mixers: Oxynator™ gas–gas mixer, KMA and SMI static mixers

H. Barrué [a], A. Karoui [a], N. Le Sauze [a,*], J. Costes [a], F. Illy [b]

[a] *Laboratoire de Génie Chimique, UMR CNRS 5503, 18 Chemin de La Loge, 31078 Toulouse Cedex 4, France*
[b] *Air Liquide, Direction Recherche et Développement, Centre de Recherche Claude Delorme, 1 Chemin de la Porte des Loges, BP 126, Les Loges en Josas, 78354 Jouy en Josas Cedex, France*

Received 20 May 2000; accepted 29 November 2000

Abstract

In this paper, a new gas–gas mixer, Oxynator, is characterized. The performance of this mixer is compared with two static mixers: Sulzer SMI and Chemineer KMA. In order to study these three gas–gas mixers, first the pressure drop is measured. Secondly, the mixing efficiency is characterized by laser sheet visualizations at the outlet of the mixer. The hydrodynamics and turbulence induced by the mixers are then measured by laser Doppler anemometry (LDA).

The purpose of this work is to understand the aerodynamics and the mixing mechanisms of the Oxynator mixer and to compare it with two static mixers. The mixing mechanisms of the Oxynator are very particular. The Oxynator creates eight swirls and a center zone, each zone increasing in space when they go away the injector. The homogeneity is reached when the zones meet and form a single zone. The intensity of turbulence created by this mixer is greater than the turbulence created by the other mixers and the pressure drop is minimum (lower than KMA and equal to SMI). The particularity of this mixer is that there is no impact between the secondary flow and the tube. The influence of flow rate on flow pattern is determined.

Keywords: Aerodynamics; Oxynator; KMA and SMI static mixers

1. Introduction

Chemical plants operation has been improving for 20 years, enhancing energy efficiency, catalyst life, selectivity and yield in order to achieve higher production at lower cost. High selectivity catalysts fully achieve their goal when reactant distribution can be known at their surface. Homogeneous distribution is preferred as far as operability of equipment is concerned. For a long time gas–gas mixing was considered as a straightforward operation, easy to design and operate. It is now recognized that this operation is not as simple as it might first appear. The general design principles established in the past could be significantly improved by taking into account the complex flow structures and the geometry of the various mixing systems.

Low viscosity fluid flow is usually turbulent, but not enough to fully eliminate inhomogeneities of concentration or temperature within short lengths of empty pipe when injection is standing alone. As an example, from a coaxial injection device, to obtain a homogeneous mixture, characterized by only 1% standard deviation from the mean concentration, a length of about 100 diameters is needed [1]. Moreover, relatively stable stream layers may be formed if the fluids, especially in the case of gases, exhibit differences in density. Consequently, a long pipe is required to homogenize the fluid (in concentrations and/or temperature). However, short mixing lengths are required when limited space is available. Suitable high efficiency mixing equipment must be developed with particular attention to low pressure drop.

Debottlenecking operations with oxygen injection may be one way of improving both process yield and costs, but catalyst, other pieces of equipment, and operability range should be addressed: whereas operation may be running smoothly at the new mean oxygen concentration (typically between 22 and 28%), operators may want to assess that there is no local oxygen content peak where specifications are not met any longer. Static mixers, which are commonly used in continuous fluid mixing, often answer to these specifications. Another kind of mixer has been developed by Air Liquide in order to be implemented on an existing compact unit with oxygen injection: the Oxynator™. It has been designed

* Corresponding author. Tel.: +33-5-61-14-89-62; fax: +33-5-61-14-89-36.
E-mail address: lesauze@gch.iut-tlse3.fr (N. Le Sauze).

1385-8947/01/$ – see front matter
PII: S1385-8947(01)00128-0

Nomenclature

D	tube diameter (m)
I	turbulence intensity (%)
L	tube length (m)
$Q_{1,2}$	principal, secondary air flow rate ($m^3\,s^{-1}$)
r	radial position (mm)
Re	Reynolds number
$RMS_{Z,r,\theta}$	root mean square velocity: axial, radial, tangential ($m\,s^{-1}$)
S	tube area (m^2)
V_{mean}	mean velocity in the empty tube ($m\,s^{-1}$)
$V_{Z,r,\theta}$	axial, radial, tangential velocity ($m\,s^{-1}$)
$Z_{0,1,2,3}$	axial positions

Greek letters

λ	adimensional pressure drop
μ	dynamic viscosity (Pa s)
θ	angular position
ρ	density ($kg\,m^{-3}$)

to minimize pressure drop and maximize mixing efficiency over a very short length with easy retrofit.

The purpose of this work is to study the aerodynamic characteristics of this gas–gas mixer in order to better understand the mixing mechanisms of this apparatus. The acquired knowledge in liquid–liquid mixing characterization is transferred and adapted to gas specificities. The aerodynamic and efficiency of mixing of the Oxynator is then compared with two static mixers: the Sulzer SMI mixers, which is commonly used in gas mixing, and the Chemineer KMA which is often encountered for viscous fluid mixing but was proposed for this application by the manufacturer.

The choice of these static mixers has been done by manufacturer regarding the specificities, the pressure drop and the cost. The SMI static mixer is a standard mixer that allows to mix miscible fluids in turbulent region. Sulzer also produces the SMV, for which efficiency in gas mixing is high [2], but which is with a greater cost.

The KMA static mixer was originally developed for laminar flow mixing but it has commonly been used for gas–gas mixing in turbulent regime too. For turbulent flow, an other static mixer developed by Chemineer, the HEV static mixer exists. The performance of this static mixer has been studied by Fasano [3], Myers et al. [4] and Bakker and Cathie [5].

The purpose of this work is not do an inventory of all the mixers and determine the most efficient in turbulent gas mixing, but to determine the mixing mechanisms of the Oxynator and to give some elements of comparison with others mixing mechanisms.

In order to do this comparison, Sulzer SMI and Chemineer KMA, standard static mixers commonly used in gas mixing, regarding their efficiency and cost, are chosen.

For more information about performance of several static mixers — pressure drop, stretching, mean shear rate and mixing efficiency — one can be reported to Rauline et al., who investigate hydrodynamic and mixing characteristics of several static mixers in laminar flow [6]. Only a few information about mixing efficiency in turbulent flow in static mixers is given in [7,8].

2. The mixing apparatus

The experimental device is composed of a 1000 mm long glass tube of 100 mm diameter (Fig. 1). A blower provides the principal air stream Q_1 with a flow rate ranging from 300 to 500 $N\,m^3\,h^{-1}$, while compressed air is supplied for secondary air with a flow rate Q_2 from 10 to 25 $N\,m^3\,h^{-1}$. The injection of the secondary flow rate is performed by a coaxial tube, 10 mm in diameter. Mixing is performed at atmospheric pressure and temperature ranging from 25 to 50°C, in the following flow conditions: $Q_1 = 300\,N\,m^3\,h^{-1}$ and $Q_2 = 10\,N\,m^3\,h^{-1}$, which corresponds to the nominal conditions noted 10/300 $N\,m^3\,h^{-1}$. The Reynolds number, $Re = DV_{mean}\rho/\mu$, is 82 000. So the regime is fully turbulent. The nominal condition is determined in order to avoid the impact of the secondary stream jets on the tube wall. For a given value of the ratio $\rho_2 V_{axial2}/\rho_1 V_{axial1}$, the impact point between the jet trajectory and the principal stream is calculated by the Abramovitch regression [9]. The nominal condition corresponds to a ratio $\rho_2 V_{axial2}/\rho_1 V_{axial1}$ giving a good location of the impact point, i.e. close to the tube wall, but without touching it. The theoretical value has been verified by the manufacturer with an experimental study. When both fluids are the same (same temperature and density), optimal condition can be expressed by V_{axial2}/V_{axial1} or directly by Q_2/Q_1. The influence of flow conditions are studied, the other flow conditions used are 7.5/300 and 15/300 $N\,m^3\,h^{-1}$.

Oxynator is adapted on the coaxial tube and achieves both injection and mixing. Static mixers are located 2 cm after the exit of the coaxial tube (Fig. 1b).

Oxynator is a hollow cylinder, 2 cm in length and 1 cm in diameter (Fig. 2a). The left extremity is open and connected to the coaxial tube which provides the gas to be mixed. On the right extremity, the cylinder section is closed. The gas leaves were located perpendicularly through a circular orifice 2 mm in width just before the section wall. A tangential movement is given to the flow by eight static blades uniformly distributed on the closure section of the cylinder (Fig. 2b). With this apparatus, the injection occurs in the radial direction of the primary flow.

The Sulzer SMI and the Chemineer KMA have a diameter equal to the tube diameter (100 mm) and have lengths of 480 and 454 mm, respectively. The SMI mixer consists of two sets of mixing elements, some kind of baffles, welded on a tube (Fig. 2c). The KMA has twisted tape inserts (Fig. 2d). The tape are twisted through 180° and abut one another at a 90° angle providing successive right- and left-hand rotation to the fluid elements. As mentioned previously, the kind of static mixers as well as their dimensions have been

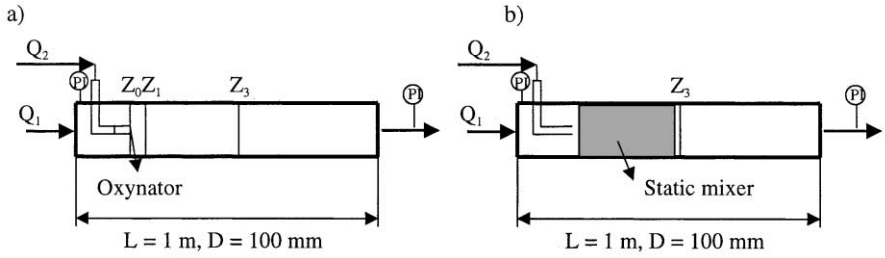

Fig. 1. Experimental device: (a) Oxynator; (b) static mixer.

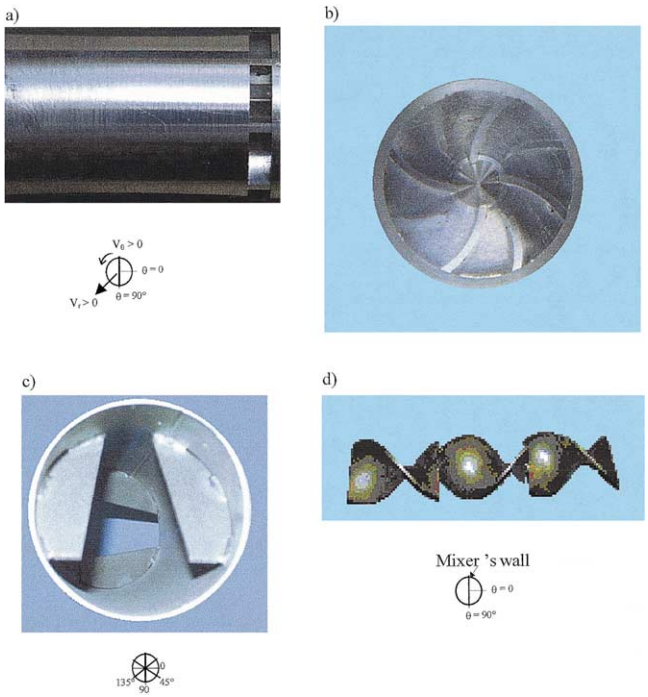

Fig. 2. Mixers slides: (a) Oxynator, longitudinal view; (b) Oxynator, top view; (c) SMI static mixer; (d) KMA static mixer.

determined by each manufacturer, to obtain a standard deviation lower than 2% (homogeneity is generally assumed in industrial application for a standard deviation lower than 5%) at the outlet of the mixer at the specified flow rates, pressure and temperature.

3. Measurements

For the three mixers, the pressure drop is measured on the main flow with water manometers, giving differential pressure versus atmospheric pressure at each end of the tube (Fig. 1).

In a second step, the mixing efficiency is characterized by laser sheet visualizations. The injected gas flow is seeded with paraffin oil droplets (refraction index = 1.4679, mean diameter $d_{32} = 3.5\,\mu m$). A laser sheet allows visualization of the droplets distribution on a pipe section. When a difference in droplets density on a measuring section is no longer observed, homogeneity is assumed. This visual observation does not give quantitative value on mixing, and the standard deviation cannot calculated from the laser sheets. But the visualizations allow to notice high and low concentrations in tracer on a section, and thus allow to understand mixing mechanisms and to compare, if the observer is always the same, different sections for different mixers.

The mixing mechanism of the Oxynator is highlighted by several laser sheets located from the outlet of the mixer to 250 mm downstream of it. Laser sheets at the outlet sections of the Chemineer and Sulzer mixers allow comparison with the Oxynator mixer.

Velocity and root mean square velocity measurements are then performed by laser Doppler anemometry (LDA). This is a well-known technique in our laboratory, which has been successfully used for the hydrodynamic characterization of stirred vessels [10] and continuous mixing devices [11,12]. It is a non-intrusive method, which requires particles that can scatter the incident light in the gaseous stream. It is difficult to find an efficient seeding in gaseous streams. Some authors have used solid particles seeding by the aide of fluidized bed [13]. We choose to seed the secondary flow with liquid droplets. A seeding generator (DISA) provides paraffin oil droplets (Risella 15, Shell).

Experiments are performed in forward scatter mode in order to obtain an analyzable signal. The laser bench is composed of the following elements:

- an ionized argon laser source (Spectra Physics) with power of 4 W;
- an optic part including a color separator, a ray divider, a Bragg cell and an optic fiber to transmit the beam;
- an emitter and a receiver equipped with the appropriate lens;
- a photomultiplier connected to the receiver;
- a flow velocity analyzer (Dantec) which allows the processing of the Doppler signal;
- an oscilloscope to control the quality of signal;
- a computer equipped with the software Floware for data processing.

For the three mixers, velocities and RMS velocities are measured in the three directions: axial, radial and tangential. It is impossible to perform measurements close to the wall of

Table 1
Pressure drops induced by mixers at nominal conditions (Q_{total} = 310 N m^3 h^{-1}, $\rho_{normal\ conditions}$ = 1.2928 g l^{-1})

	Oxynator	KMA static mixer	SMI static mixer
ΔP (mbar)	2.6	4.3	2.6
λ	3.346	5.534	3.346

the tube, i.e. at less than 5 mm, because of the deformation of the laser beam in this region.

4. Results and discussion

4.1. Pressure drop

The pressure drop of gas–gas mixers is measured at the nominal flow rate. In order to account for the pressure drop due to the mixer, the pressure drop corresponding to the coaxial injection is measured and deduced to the total pressure drop. The pressure drop for a coaxial injection is 2.4 cm of water (i.e. 2.4 mbar).

Table 1 gives the pressure drops induced by the mixers. λ is a dimensionless way to characterize the pressure drop. It is calculated by

$$\lambda = \frac{\text{pressure drop}}{\rho V_{mean}^2/2} \quad (1)$$

The Oxynator and the SMI static mixer produce the same pressure drop equal to 2.6 mbar. Therefore, in an industrial process, the use of these mixers will not produce great energy dissipation.

The KMA static mixer has a pressure drop at 4.3 mbar; which is 1.65 times more than that produced by the Oxynator and SMI static mixer. This mixer dissipates more power than the other mixer systems. The pressure drop per length unit of static mixer can be calculated for SMI and KMA. Values are 5.4 and 9.5 mbar m^{-1}, respectively, for SMI and KMA. For the Oxynator, this information is not useable because mixing is not performed in the mixer but downstream of the mixer. A good comparison with both other mixers could be the pressure drop per mixing length unit, which is a parameter to be determined in this work.

4.2. Laser sheet visualizations

In order to show the mixing mechanisms of each mixer, laser sheet visualizations are given. Firstly, experiments are performed in an empty pipe, with a coaxial injector and without any mixing system. Fig. 3 shows the visualizations located at 0, 50, 100 and 150 mm of the injection. The injection diameter is 1 cm (Fig. 3a). At 50 mm, the zone with oil has a diameter equal to 3 cm. At 150 mm, the oil occupies a circular area which a diameter equals only half of the tube diameter. Clayton et al. [1] show that to obtain a homogeneous mixture, a length of about 100 diameters is needed.

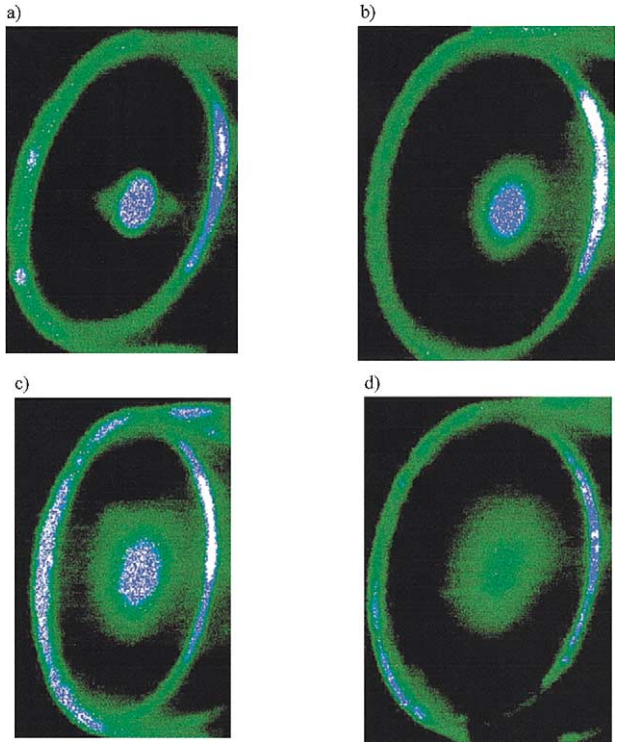

Fig. 3. Laser sheet visualizations for the coaxial injection and flow rates 10/300 N m^3 h^{-1}: (a) 0 mm; (b) 50 mm; (c) 100 mm; (d) 150 mm.

For the Oxynator, the mixing evolution along the tube can be clearly observed on the five laser sheets located at 0, 20, 50, 100 and 150 mm of the outlet. For the nominal flow rate, the sheets are given in Fig. 4. The secondary flow is divided in eight jets at the outlet of the mixer. At this flow rate conditions, there is no impact of the jets on the wall of the tube (Fig. 4a). Impact has to be avoided in industrial applications dealing with oxygen introduction: it could bring about inflammation resulting from the reaction of oxygen present at high concentration with deposit on the tube wall. Jets are about 20 mm in length and are oriented in the same direction as the Oxynator blades, i.e. counterclockwise. At Z_2 = 20 mm, an interesting phenomenon is observed (Fig. 4b): the jets are transformed in swirls. The tangential movement is in the opposite direction from the initial movement noticed at Z_0 = 0 mm. The swirls are connected to a central disc with small passages. In the central disc, the tracer concentration seems to be homogeneous and lower than in the jets. The swirls can be observed up to 50 mm from the injection and the diameter of the swirls increases. At 50 mm, Fig. 4c, the swirls have increased and are close to the wall. After 50 mm, the swirls disappear and the tracer repartition becomes more homogeneous (Fig. 4d). Homogeneity is then achieved by turbulent diffusion. At Z = 150 mm, the tracer appears to be homogeneously distributed in the tube (Fig. 4e), and no more evolution of the tracer repartition is observed after this section. It has to be noticed that the high intensity zones on Fig. 4e are due to reflecting effects, and not to higher concentrations.

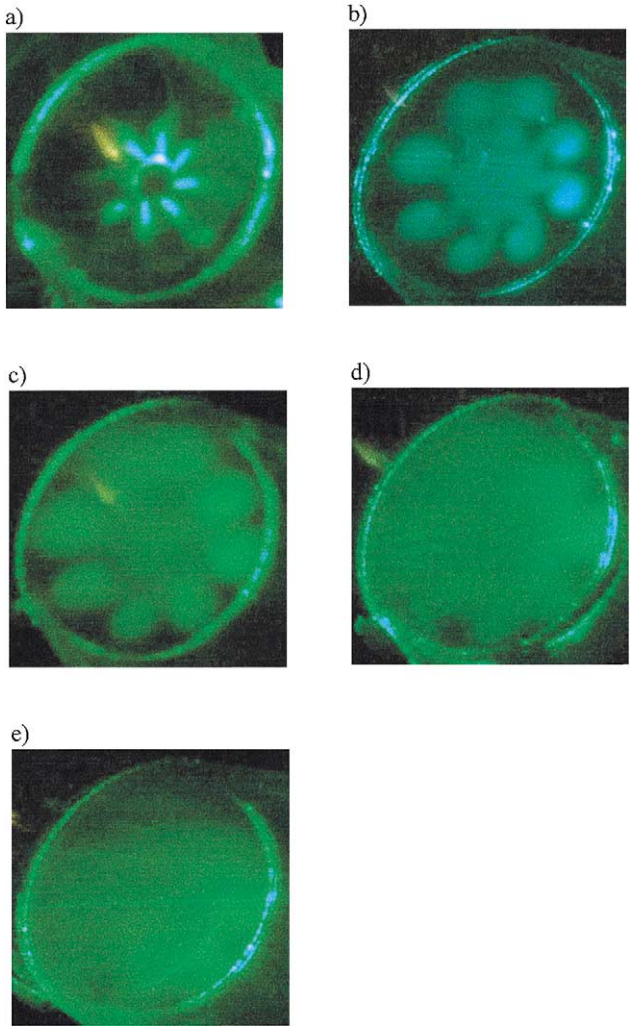

Fig. 4. Laser sheet visualizations for the Oxynator mixer and flow rates 10/300 N m^3 h^{-1}: (a) 0 mm; (b) 20 mm; (c) 50 mm; (d) 100 mm; (e) 150 mm.

At a given length from the injection point, the homogeneity is more greater with Oxynator than with the coaxial injection: at $Z = 150$ mm, the homogeneity is visually obtained. At the same distance from the coaxial injector, the oil occupies only half of the tube.

The manufacturer recommends to use the Oxynator with flow rates included between 8/300 and 12/300 N m^3 h^{-1} (variation of ±20%). It is interesting to notice the effect of secondary flow rate variation on the mixing efficiency. Two other conditions have been studied: 15/300 N m^3 h^{-1}, which is higher than the limit given by the manufacturer (+50%) and 7.5/300 N m^3 h^{-1} which is lower than the limit given by the manufacturer (−25%).

If the secondary flow rate is greater, for flow rate conditions 15/300 N m^3 h^{-1}, Fig. 5, the initial jets are greater than for the first flow rate (length of about 30 mm). At 20 mm (Fig. 5b), the swirls reach the tube. At 100 mm, the oil tracer occupies all of the section. Homogeneity is reached more quickly than for the nominal flow rate. However, one of the

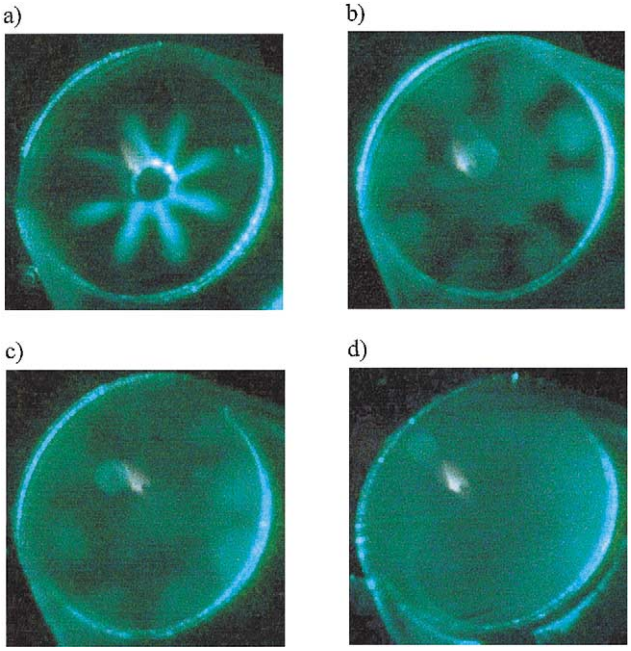

Fig. 5. Laser sheet visualizations for the Oxynator mixer and flow rates 15/300 N m^3 h^{-1}: (a) 0 mm; (b) 20 mm; (c) 50 mm; (d) 100 mm.

advantages of this mixer is that the secondary flow does not create impact on the wall. In this case there is some impact so the flow rate is not suitable, even if the mixing efficiency is high.

If the conditions are 7.5/300 N m^3 h^{-1}, Fig. 6, the initial length of the jets is about 12 mm. The swirls develop less than for the nominal conditions and they disappear before the length of 50 mm, Fig. 6c. At 50 mm, the oil is not located in the entire tube section. At 100 mm, the section occupied is about 60 mm diameter, i.e. 36% of the tube section. It is a diameter more important than for the co axial injection at 150 mm (50 mm). The area occupied by the tracer will then increase very slowly.

In that conditions, the Oxynator is more efficient than the coaxial injection, but the mixing length is greater than for the flow rate 10/300 N m^3 h^{-1}. The nominal flow rate is the optimum condition to obtain an efficient mixing without an impact of the secondary flow on the tube. If the manufacturer nominal flow rate is not respected, with an acceptable variation of secondary flow rate inferior to 20%, mixing efficiency will be drastically decreased (for a secondary flow rate too low) or wall impact will not be avoided (for a secondary flow rate too high).

In order to compare the mixing efficiency of KMA and SMI with the mixing efficiency of Oxynator, a laser sheet has been made at the outside of both static mixers (Fig. 7). These visualizations are difficult because the brightness is poor. In both the cases, the tracer appears to be homogeneously distributed on the whole section. No evolution of the tracer repartition is noticed downstream of this section, which confirms that the homogeneity corresponding to our visual criterion is reached.

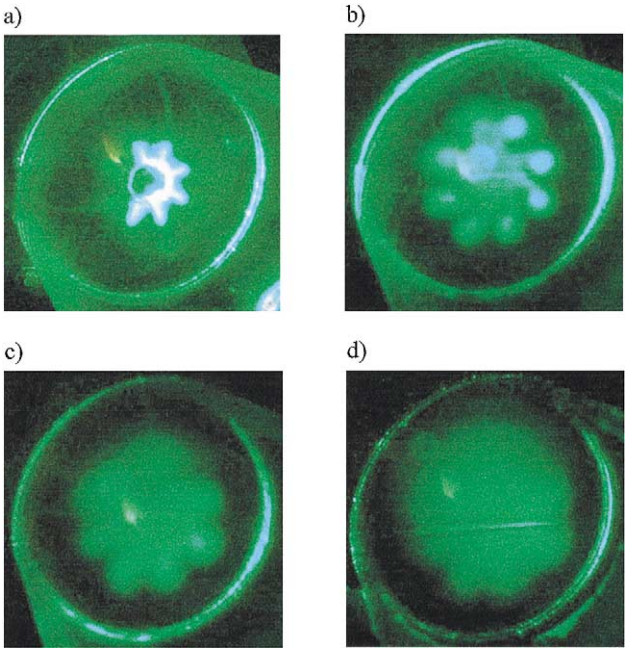

Fig. 6. Laser sheet visualizations for the Oxynator mixer and flow rates 7.5/300 N m^3 h^{-1}: (a) 0 mm; (b) 20 mm; (c) 50 mm; (d) 100 mm.

No influence is noticed at other flow rates. The homogeneity is always reached for flow rate between 7.5/300 and 15/300 N m^3 h^{-1}. For KMA and SMI static mixer, the global homogeneity is obtained at the outlet, i.e. at around 500 mm of the injection. We do not have information about the mixing evolution along the mixers. The homogeneity can be obtained before the outlet, and it would be necessary to do intermediate laser sheets to determine the real mixing length. In our case, this study has been impossible to realize: SMI mixer is in stainless steel and is not transparent, KMA mixer walls create reflecting zones and dark zones, which do not permit to obtain significant visualizations.

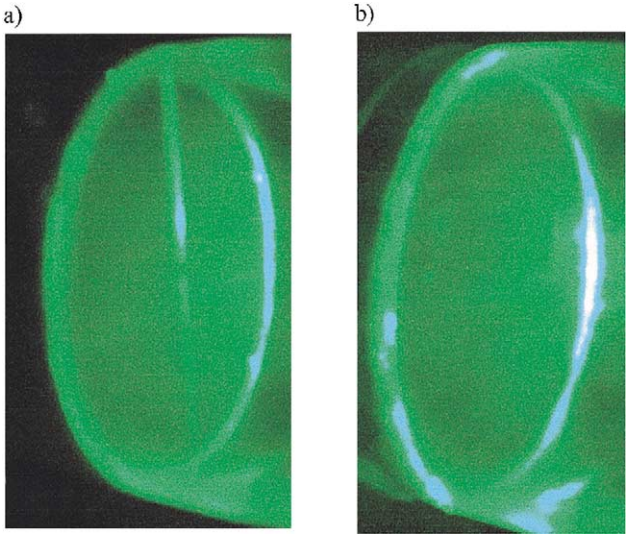

Fig. 7. Laser sheet visualizations for flow rates 10/300 N m^3 h^{-1} at the outlet of (a) the KMA static mixer and (b) the SMI static mixer.

The mixing mechanisms cannot be observed along these mixers, but it is well known for the KMA in laminar flow [14,15] and described in technical notice for the SMI [16]. In a turbulent flow, the mixing in the three mixers is due to a complex flow pattern. To understand this flow pattern, LDA measurements are performed.

4.3. Aerodynamics characterization

The aerodynamics in terms of velocity, RMS and turbulence intensity generated by each mixer is characterized. LDA measurements are made on several planes, Fig. 2 shows for each mixer the measurement angular positions. The tangential velocity is positive for counterclockwise and the radial velocity is positive when the air is flowing from the center towards the wall. The velocities are divided by the mean velocity in the empty tube (V_{mean}) to compare results with different flow rates.

$$V_{\text{mean}} = \frac{Q_1 + Q_2}{S} \tag{2}$$

4.4. Oxynator mixer

For the Oxynator mixer, one eighth of the tube is studied: the mixer is composed of eight similar blades and it has been established on several measurement points that the flow pattern can be duplicated. Measurements are carried out on three half axes of the three sections Z_1, Z_2 and Z_3, respectively, located at 10, 20 and 500 mm downstream of the mixer. It is difficult to do measurements near the outlet due to the finger jets and reflection. Fig. 8 shows the axial, radial and tangential velocities at Z_1. For a given radius, velocities are similar for $\theta = 0$ and 45°, angles which correspond to the location of the blades. Axial velocities are smaller for $\theta = 22.5°$, which corresponds to the median angle between two blades. The maximum axial velocity is 1.7 times more than the mean velocity in the empty tube. The evolution is the same for the three angles. They are negative from the center of the tube ($V_Z/V_{\text{mean}} = -0.9$ for $r = 0$ mm) to $r = 11$ mm, where $V_Z/V_{\text{mean}} = 0$. They increase from $r = 11$ to 25 mm ($V_Z/V_{\text{mean}} = 1.7$ for $r = 25$ mm) and decrease thereafter. The jet length is 30 mm. The center zone observed in laser sheet visualizations corresponds at a negative axial velocity. So there is a recirculation of the flow in the tube center.

Radial velocities (Fig. 8b) are quite similar for each angle from $r = 0$ to 17 mm. From 0 to 11 mm, V_r are slightly positive (close to $0.1V_{\text{mean}}$). From 11 to 17 mm they are negative, with the highest absolute value between $0.15V_{\text{mean}}$ and $0.2V_{\text{mean}}$ for $r = 15$ mm. After 17 mm, their evolution versus r is different between $\theta = 22.5°$ and $\theta = 0$ and 45°. The higher radial velocities are obtained for the median

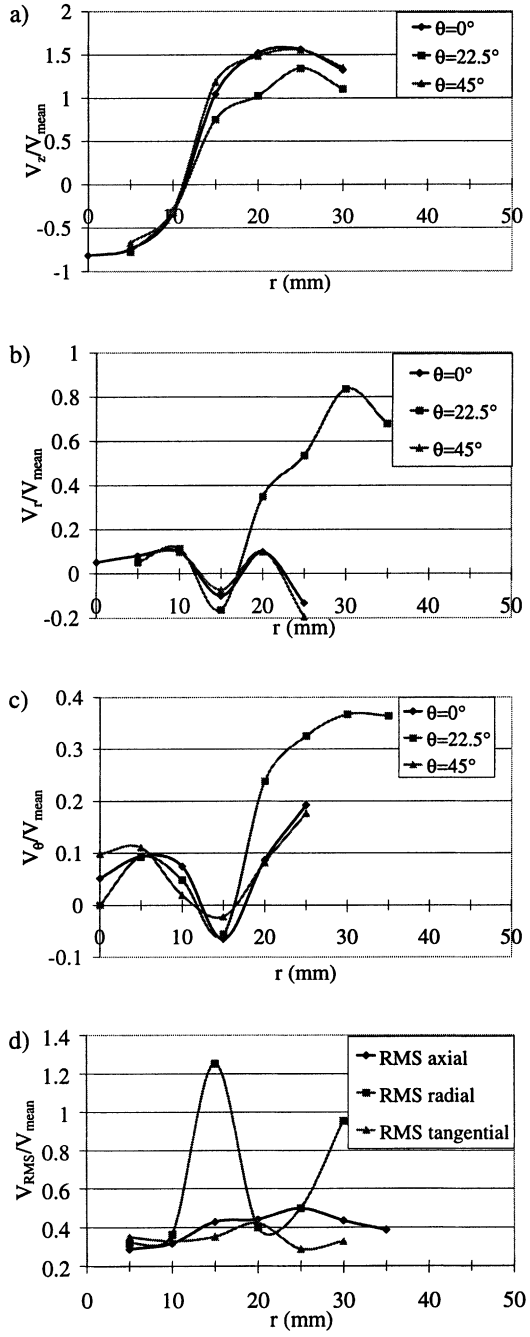

Fig. 8. Oxynator velocities at $Z_1 = 10$ mm: (a) V_Z; (b) V_r; (c) V_θ; (d) RMS ($\theta = 0°$).

position. The maximum value is equal to $0.8V_{mean}$ for $r = 30$ mm, for the jet tip. For $\theta = 0$ and 45°, the radial velocity is near zero. Tangential velocities (Fig. 8c) have an evolution versus r similar to radial velocities: same values, close to $0.1V_{mean}$, for each angle from $r = 0$ to 17 mm, negative values between 11 and 17 mm and a different evolution, after 17 mm, between 22.5° and the other angles. The higher tangential velocity equal to $0.38V_{mean}$ is obtained for $\theta = 22.5°$ and $r = 30$ mm.

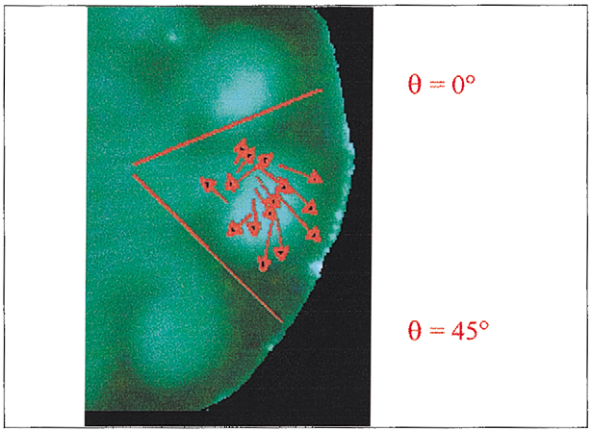

Fig. 9. Representation (V_r, V_θ) of the velocity at $Z = 20$ mm after the Oxynator.

The Oxynator creates a depression zone, which can be characterized by the velocity measurements performed on a transversal section located 10 mm downstream from the mixer. At this distance, the diameter of the depression zone is around 20 mm — two Oxynator diameter. In that zone, axial velocities are negative. The highest absolute value, from the same order of magnitude than the mean velocity (V_{mean}), is situated at the center. Axial velocity decreases from the center to the periphery of the zone. Radial and tangential velocities are positive and low. Radial velocities are constant and close to $0.1V_{mean}$. Tangential velocities are maximum at $r = 5$ mm, more or less constant for $\theta = 0$ and 45°, increasing for $\theta = 22.5°$ from $r = 0$ to 5 mm, decreasing at each angle from $r = 5$ to 11 mm. In a ring 5 mm in depth located around the depression zone, axial velocities become positive when radial and tangential velocities become negative. In the last annulus, the axial movement is predominant, except for $\theta = 22.5°$ where the radial and tangential velocities are quite high. Flow differences between $\theta = 22.5°$ and $\theta = 0$ and 45° can be explained by the geometry of the Oxynator: the blades are located at 0 and 45°, when 22.5° corresponds to the median position between two blades. The rotational movement is then maximum between the blades. For these measurements located at 10 mm of the outlet, velocities located at 22.5° characterize the jets of secondary flow. In the jets, the radial velocity is the same order of the mean axial velocity in the empty tube.

In order to characterize the local movement in the swirls, some additional measurements located on one swirl have been made. A vertical plane located at 20 mm of the outlet of the mixer where swirls are fully developed is studied. Measurements are made on five angular positions between 11.25 and 33.75°. Fig. 9 shows the radial and tangential velocities on this vertical plane. This velocity field confirms the presence of swirls and explains the tracer repartition. When r increases, the tangential velocity is first positive, with a maximum of $0.25V_{mean}$, and after negative with a maximum of $-0.4V_{mean}$. Radial velocities are included between $-0.25V_{mean}$ and $0.36V_{mean}$.

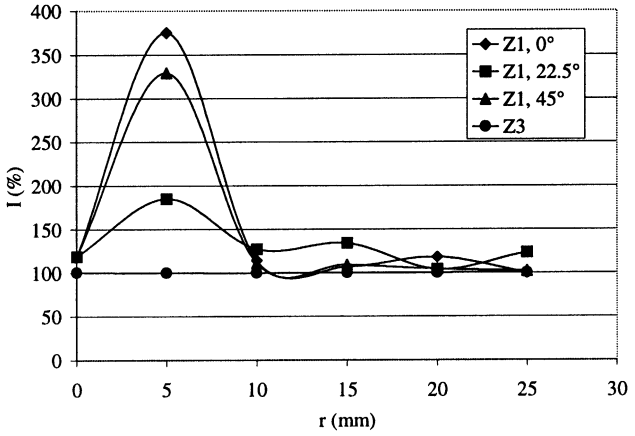

Fig. 10. Intensity of turbulence downstream of the Oxynator.

RMS velocities have been measured in the jet (Z = 10 mm) at the same position than velocities. No significant difference can be noticed versus the angular position. An example of axial, radial and tangential RMS at $\theta = 0^\circ$ is given on Fig. 8d. Axial values range from $0.3V_{\text{mean}}$ to $0.5V_{\text{mean}}$, $0.4 < \text{RMS}_r/V_{\text{mean}} < 1.3$ with a maximum at $r = 15$ mm and tangential $\text{RMS}_\theta = 0.4V_{\text{mean}}$. If RMS_Z and RMS_θ are of the same order of magnitude, RMS_r values are higher. The maximum is noticed for $r = 15$ mm so on the periphery of the depression zone. The turbulence promoted by the Oxynator is then anisotropic.

Fig. 10 gives the turbulence intensity I versus r at Z_1 = 10 mm and $Z_3 = 500$ mm. I is calculated by

$$I = \frac{\sqrt{\text{RMS}_r^2 + \text{RMS}_\theta^2 + \text{RMS}_Z^2}}{\sqrt{V_r^2 + V_\theta^2 + V_Z^2}} \quad (3)$$

The turbulence is very high: $75\% < I < 375\%$ at Z_1. The intensity is maximum for $r = 10$ mm at all the angular position, which corresponds to the borderline of the depression zone. The turbulence intensity values are very different versus the angle for $r = 10$ mm: the maximum value is obtained at $\theta = 0^\circ$ ($I = 375\%$) and the minimum value is obtained at $\theta = 22.5^\circ$ ($I = 180\%$).

Going away the Oxynator, the velocities become homogeneous versus r. No more difference appears versus the angular position. At $Z_3 = 500$ mm (Fig. 11), axial profile is close to the universal profile in turbulent regime. Radial and tangential velocities are small (less than $0.14V_{\text{mean}}$). The lowest radial velocities are situated in a central disc of a tube, 10 mm in diameter. In the other part of the tube, V_r is constant and close to $1.3V_{\text{mean}}$. Tangential velocities decrease from $1.25V_{\text{mean}}$ in the center of the tube to 0 for r = 40 mm. At Z_3, RMS are the same in the three directions and do not depend on r or θ. The mean value of RMS is close to $0.1V_{\text{mean}}$. Turbulence intensities are reported on Fig. 10. I is equal to 88% for all the angular positions which is much higher than the turbulence intensity in an empty tube, close

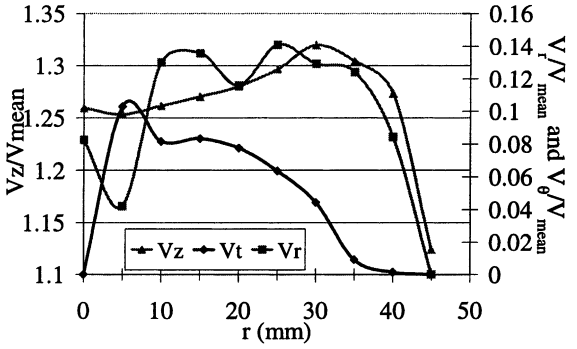

Fig. 11. Oxynator velocities at $Z_3 = 500$ mm ($\theta = 22.5^\circ$).

to 20% for a turbulent regime. At this distance, even if the universal axial profile is obtained, the Oxynator still influences the flow which achieves a rotational movement and an important turbulence degree.

These different velocity measurements inform us on the flow pattern at the outlet of the mixer and so on the mixing mechanisms. The Oxynator divides the secondary flow in eight jets. In these jets, the axial velocity is less important than in the rest of the flow, the radial velocity is maximum at the jet tip and the tangential velocity is positive. Quickly (between 10 and 20 mm), jets are transformed into eight swirls connected to the central disc with small passages. The maximum of turbulence is created at the periphery of the center zone. Each zone increases in space, and the homogeneity is reached when the zones meet and form a single zone.

Some measurements are performed for the flow rate 7.5/300 N m^3 h^{-1}. Fig. 12 shows the velocities difference between the two flow rate for $\theta = 22.5^\circ$ and $Z = 10$ mm. The location of the measurements is in the jet. Axial velocities (Fig. 12a) are similar and radial velocities are different (Fig. 12b). For 7.5/300 N m^3 h^{-1}, the maximum is $0.6V_{\text{mean}}$ (0.8 for 10/300 N m^3 h^{-1}) and is obtained at $r = 20$ mm ($r = 30$ mm for 10/300 N m^3 h^{-1}). The radial velocity is lightly negative at 10 mm. The tangential velocity profile is different. Tangential velocities (Fig. 12c) are always positive and the maximum value is $0.25V_{\text{mean}}$ at $r = 20$ mm. So, the length of the jet is 20 mm for the flow rate 7.5/300 N m^3 h^{-1}, it is smaller than the previous one. The periphery of the center zone is not so perturbed than for the flow rate 10/300 N m^3 h^{-1}. RMS velocities are low for the flow rate 7.5/300 N m^3 h^{-1}. The maximum equal to $0.65V_{\text{mean}}$ is obtained for $r = 20$ mm in axial direction. The maximum turbulence intensity is 300% and at $Z = 500$ mm the value is 25%. In this case the turbulence intensity decreases quickly in the tube.

4.5. KMA static mixer

The purpose of this work is not to fully study this kind of mixers but to give some comparison elements with Oxynator, in term of aerodynamic characterization and mixing mechanisms.

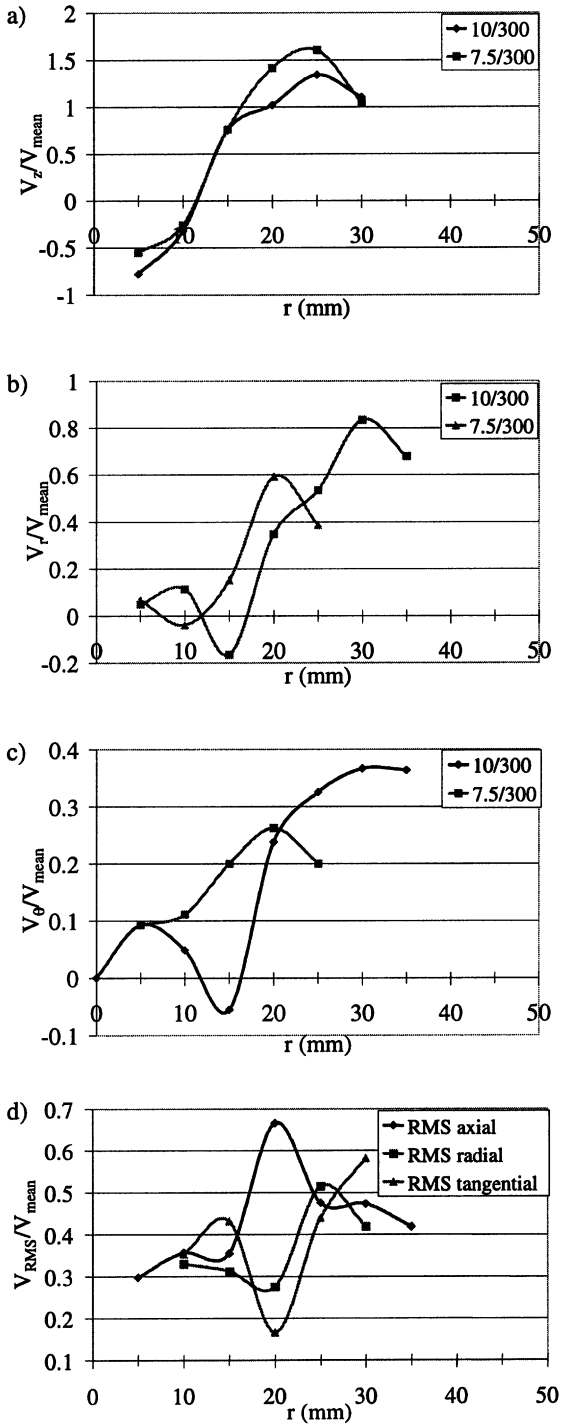

Fig. 12. Oxynator velocities at $Z_1 = 10\,\text{mm}$ and $\theta = 22.5°$: (a) V_Z for a flow rate of 7.5/300 and 10/300 N m^3 h^{-1}; (b) V_r for a flow rate of 7.5/300 and 10/300 N m^3 h^{-1}; (c) V_θ for a flow rate of 7.5/300 and 10/300 N m^3 h^{-1}; (d) V_{RMS} for a flow rate of 7.5/300 N m^3 h^{-1}.

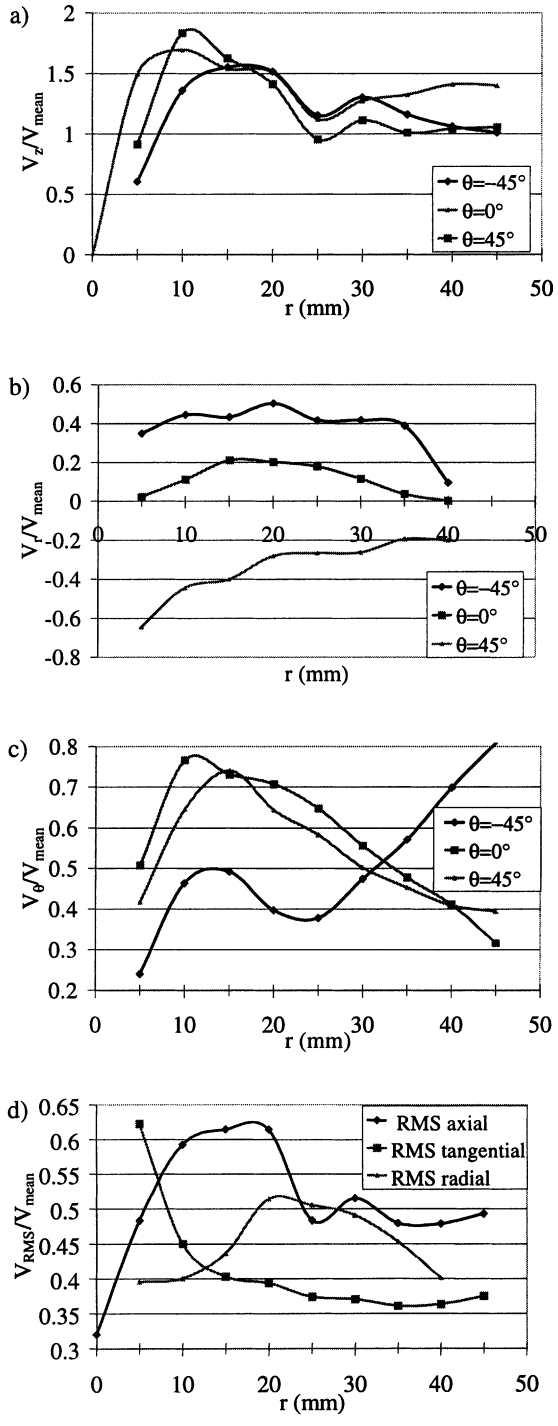

Fig. 13. Velocities at the outlet of KMA: (a) V_Z; (b) V_r; (c) V_θ; (d) RMS ($\theta = -22.5°$).

The aerodynamic of the KMA mixer is characterized at the outlet of the mixer, corresponding to $Z_3 = 500\,\text{mm}$. LDA measurements inside the mixer are impossible because the mixer walls do not allow the laser ray to penetrate. Assuming that the flow is the same on each side of the mixer wall, which is based on a physical symmetry, only a half part of the outside section is studied. Measurements are carried out on nine half axes distributed from -90 to $90°$ (Fig. 2d).

Fig. 13 shows the evolution of axial, radial and tangential velocities versus r at 2 mm of the outlet of the KMA mixer, for angular positions $\theta = 45, 0,$ and $-45°$. At the outlet of

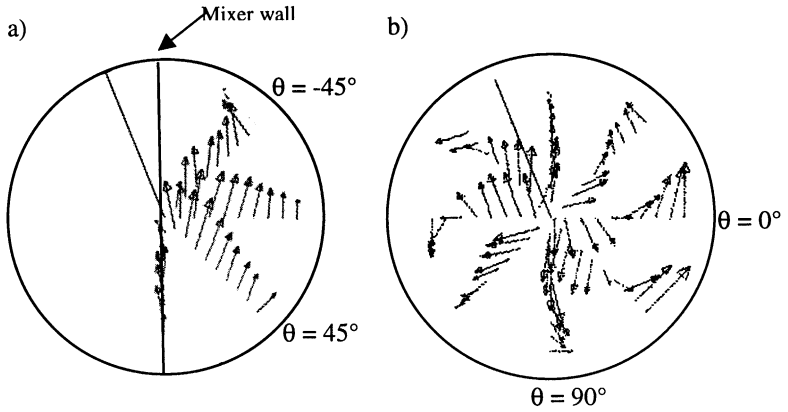

Fig. 14. Representation (V_r, V_θ) of the velocity at the outlet of (a) KMA static mixer and (b) SMI static mixer.

the mixer, the axial movement is quasi independent of the angular position although a difference of 20% is noticed at several radii. Axial velocities are small at the center of the tube corresponding to the location of the mixer wall, increase up to $1.8V_{mean}$ for $r = 10$ mm then decrease and stabilize around $1.2V_{mean}$ for r ranging from 25 to 45 mm.

Radial movement depends on the angular position: for a given radius, the closer to the mixer wall the measuring point is and the higher is the radial velocity. The sign of the radial velocities is opposite for the positive angles and the negatives angles. That means that in the upper part of the half tube, the radial movement is oriented from the center to the wall of the tube and in the lower part of the half tube, the radial movement is oriented from the wall to the center. The movement is not symmetric: V_r are higher and more regular versus r in the upper part of the tube and it is positive for $\theta = 0^\circ$. For $\theta = -45^\circ$, a mean value of $0.4V_{mean}$ is calculated for $5\,mm < r < 35\,mm$ when for $\theta = 45^\circ$, in the same range of r, V_r varies from $-0.7V_{mean}$ to $-0.2V_{mean}$.

Tangential velocities are higher than the radial velocities. The tangential movement is different with the angle. For $\theta = 0$ and 45°, V_θ increases from the center to $r = 10$ mm, and then decreases to $r = 45$ mm. Tangential velocities are positive, ranging from $0.3V_{mean}$ to $0.8V_{mean}$. For $\theta = -45^\circ$, the tangential velocity increases from the center ($0.2V_{mean}$) to the wall ($0.8V_{mean}$).

Axial, radial and tangential RMS do not depend on θ. Fig. 13d gives an example of their evolution versus r for $\theta = -22.5^\circ$. RMS values are different versus the direction, the turbulence is then anisotropic. Values range from $0.35V_{mean}$ to $0.65V_{mean}$, giving a mean turbulence intensity I equal to 60%. A higher I has been calculated at $r = 5$ mm, ranging from 80 to 160% versus the angle of measure. It can be explained by the small velocities measured on this section.

A representation in the vertical plane of the radial and tangential velocities is done (Fig. 14a). In this figure, the rotational movement of all the flow can be observed. At $\theta = 45^\circ$, the flow goes towards the center and at $\theta = -45^\circ$ the flow goes towards the wall.

It can be concluded that the KMA promotes a quasi-homogeneous flow, with an important rotational movement. In this static mixer, a first element divided the flows in two parts, which are symmetric and have a regular rotational movement. In each part, the mixing is first created by this rotational movement, second enhanced by the turbulence. The two parts of the flow are then recombined in a second element of mixing.

4.6. SMI static mixer

Due to the stainless steel walls, velocities cannot be measured by LDV in the SMI mixer and the flow is only characterized at the outlet of the mixer, at $Z_3 = 500$ mm. Measurements are carried out on the whole section, on four axes distributed from -90 to 90° (Fig. 2c).

No symmetry is noticed in this static mixer. The velocity depends on the angular position. Fig. 15 shows the velocities in three axes ($\theta = -45$, 0 and 45°). Velocity values are similar for $\theta = -45$ and 90° and different for $\theta = 0^\circ$. Axial velocities are nearly constant versus r for $\theta = 45$ and 90°, the value is between $1.5V_{mean}$ and $2V_{mean}$. For $\theta = 0^\circ$, axial velocities depend on r: they are maximum at the center of the tube and decrease from the center to the wall. The lowest velocities correspond to locations close to the insert walls. V_Z range from $0.5V_{mean}$ to $2V_{mean}$. Radial velocities are positive. The variation with r is not very important, but profiles are different versus θ. The lowest velocity is obtain for $\theta = 0^\circ$, and is around $0.3V_{mean}$. The maximum is equal to V_{mean} and is obtained for $\theta = 90^\circ$ so between the baffles positioned inside the tube. Tangential velocities are dependent on the radial position. Small absolute values are obtained for $\theta = -45$ and 90°, higher for $\theta = 0^\circ$. They are negative in the central part of the tube ($-30\,mm < r < 20\,mm$) and positive in the periphery zone. The maximum is obtained for $\theta = 0^\circ$ with values ranging from $-1V_{mean}$ to $1V_{mean}$. Velocities are minimum, close to 0, for $\theta = 90^\circ$.

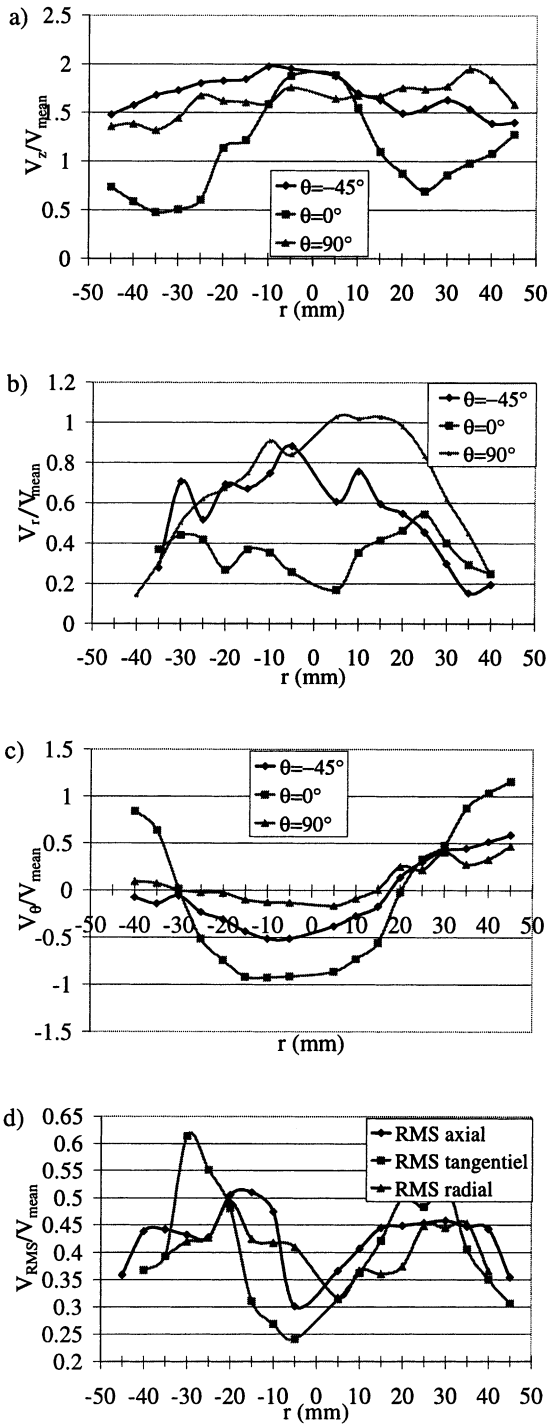

Fig. 15. Velocities at the outlet of SMI: (a) V_Z; (b) V_r; (c) V_θ; (d) RMS ($\theta = 0^\circ$).

SMI promotes a predominant axial movement, with a high radial component for each angle, and an important tangential component for $\theta = 0^\circ$. The flow pattern outside this static mixer is then very complex and fully tridimensional.

Axial, radial and tangential RMS profiles are identical — the turbulence is then isotropic and do not depend on θ but are weakly dependent on r. Fig. 15d gives an example of their evolution versus r for $\theta = 0^\circ$. Values range from $0.25V_{mean}$ (at the center) to $0.65V_{mean}$ ($r = -30$ mm). The mean turbulence intensity I depends on θ. I is locally high ($30\% < I < 150\%$) for $\theta = 0$ and 45° and smaller for $\theta = 90^\circ$ ($20\% < I < 60\%$). High values correspond to small mean velocities.

Fig. 14b shows the movement in a vertical plane. The movement is rotational for the most part of the tube. The radial part is important, and the tangential direction changes versus r. The tangential velocity is negative (clockwise) in the central part and positive near the wall. For $\theta = 90^\circ$, the movement is only radial. The flow is not so regular than in the KMA static mixer. It is created by the baffles located on the wall of the tube, is complex and fully tridimensional. In that case, the secondary flow is not divided, mixing is only produced by complex flow pattern and turbulence, which mean intensity is a little higher than KMA turbulence intensity and smaller than the Oxynator turbulence intensity.

5. Conclusion

The three flow patterns, measured by LDA, at the outlet of the three mixers are radically different.

The KMA static mixer divides the flow in two parts and creates an important rotational movement (V_r and V_θ are close to $0.3V_{mean}$), which enhances the mixing. Turbulence is not very high in the mixers (the mean turbulence intensity is close to 60% at the outlet of the mixers).

The SMI static mixer does not divide the flow. It creates a very complex and fully tridimensional flow pattern. Turbulence intensity is fluctuating versus the angle, mean intensity is higher than KMA turbulence intensity.

The aerodynamic characteristics of Oxynator are different. The rotational movement created downstream of the mixer is low compared to the other mixers (V_r and V_θ are close to $0.1V_{mean}$). The Oxynator creates eight swirls. Just at the outlet of Oxynator, velocities are inhomogeneous resulting in a high turbulence ($80\% < I < 375\%$). When the distance from the mixer increases, the flow becomes more homogeneous and can be quickly compared to the universal flow pattern in an empty tube in term of velocity. However, the turbulence remains important ($I = 88\%$, 500 mm downstream of the mixer).

Mixing is achieved mainly by separation of the flow in eight parts, by turbulence and to a lower extend by rotational movement of the swirls.

A comparison of mixers has to take into account several parameters:

- The mixing efficiency, which is the most important characteristic of a mixing apparatus. The efficiency required depends on the mixing quality desired for the application.
- The pressure drop, which is an important characteristic in term of cost.
- The mixing length, which is a technical characteristic often limiting in an existing process.

Homogeneity has been addressed by laser sheet visualizations. Global homogeneity is obtained with the three mixers studied, at the outlet of KMA and SMI static mixers, i.e. at 454 and 480 mm, respectively, downstream of the injection, at 150 mm downstream of Oxynator. We do not have information of the mixing quality into the KMA and SMI. It would be necessary to perform intermediate laser sheet investigations to compare more precisely the mixing length of the three mixers.

KMA and SMI lengths have been designed by the manufacturers to meet our request (S.D. = 2%). But in our study, measurement of standard deviation has not been possible. We can just conclude that homogeneity, visually determined, is comparable in the three mixing configurations.

The particularity of the Oxynator is that there is no impact between the secondary flow and the wall. This result can be a strong advantage in some industrial practices. But the optimum flow rates indicated by the manufacturer has to be respected with a difference inferior to 20%. If not, mixing efficiency is decreased (if secondary flow rate is too small), or impact is not avoided (if secondary flow rate is too high).

This work allows to understand and compare the mixing mechanisms of gas in the three mixers. The mixing is qualitatively characterized by the laser sheets visualizations. In order to do quantitative characterizations, others methods have to be developed, for example, laser-induced fluorescence and MIE diffusion [17,18].

An other possibility is to use computational fluid dynamics (CFD) to simulate the hydrodynamics and the mixing and to compare the standard deviation downstream of the injection for each mixer. CFD studies are now in progress in our laboratory to complete the experimental study presented in this article.

Acknowledgements

We would like to acknowledge several colleagues: M. Pern for her technical support, C. Faure and P. Mavros for the photographic work, as well as Air Liquide, Research and Development Department, CRCD, for their financial support.

References

[1] G.C. Clayton, A.M. Ball, R. Spackman, Dispersion and Mixing during Turbulent Flow of Water in a Circular Pipe, No. AERE-R 5569, Report of Isotope Research Division, Wantage Research Laboratory, Wantage, Berks, UK, 1968.
[2] W.A. Tauscher, F.A. Streiff, Static mixing of gases, CEP, 1979, pp. 61–65.
[3] J.B. Fasano, Kenics HEV mixer sets a new standard for turbulent flow mixing efficiency, in: Proceedings of the Mixing XIII Conference, Canada, 1991.
[4] Myers, A. Bakker, Ryan, Avoid agitation by selecting static mixers, Chem. Eng. Prog. (1997) 27–32.
[5] A. Bakker, N. Cathie, Modeling of the flow and mixing in HEV static mixers, IChemE Symp. Ser. 136 (1994) 533–539.
[6] D. Rauline, P.A. Tanguy, J.M. Le Blévec, J. Bousquet, Numerical investigation of performance of several static mixers, CJChE 76 (1998) 527–535.
[7] F.A. Streiff, S. Jaffer, G. Scheider, The design and application of static lixer technology, in: Proceedings of the 3rd International Symposium on Mixing in Industrial Processes, Japan, 1999, pp. 107–114.
[8] Static Sulzer Gas Mixers for DeNO$_x$ Plants, Mixing and Reaction Technology, No. VT 10120, Technical Information, Sulzer Chemtech.
[9] G.N. Abramovitch, The Theory of Turbulent Jets, MIT Press, Cambridge, 1963.
[10] C. Baudou, Agitation par des systèmes axiaux simples ou multi-étagés, Obtention de l'hydrodynamique par vélocimétrie laser à effet doppler, Thèse de l'INP de Toulouse, France, 1997.
[11] P. Guiraud, Mélange turbulent en réacteur tubulaire, Expériences et modélisation, thèse de l'INP Toulouse, France, 1989.
[12] A. Karoui, F. Hakenholz, N. Le Sauze, J. Costes, J. Bertrand, Determination of the mixing performance of Sulzer SMV static mixers by laser-induced fluorescence, CJChE A 7 (6) (1998) 522–527.
[13] M.C. Lai, G.M. Faetli, A combined laser Doppler anemometer/laser-induced fluorescence system for turbulent transport measurements, J. Heat Transfer 109 (1) (1987) 254–256.
[14] Th. Avalosse, M.J. Crochet, Finite-element simulation of mixing. 2. Three-dimensional flow through a Kenics mixer, AIChE J. 43 (3) (1997) 588–597.
[15] D.M. Hobbs, P.D. Swanson, F.J. Muzzio, Numerical characterization of low Reynolds number flow in the Kenics static mixer, Chem. Eng. Sci. 53 (8) (1998) 1565–1584.
[16] Sulzer Mixer SMI for Turbulent Flow, Technical Notice No. 23-96-06-40.
[17] A. Lozano, B. Yip, R.K. Hanson, Acetone, a tracer for concentration measurements in gaseous flows by planar laser-induced fluorescence, Exp. Fluid 13 (1992) 369–376.
[18] R.E. Rosensweig, H.C. Hottel, G.C. Williams, Smoke-scattered light measurements of turbulent concentration fluctuations, Chem. Eng. Sci. 15 (1961) 111–120.